Civil, Architectural and Environmental
Engineering Faculty Research & Creative Works

Civil, Architectural and Environmental
Engineering

01 Jan 2005

The Influence of Ammonia and Carbon Dioxide on the Sorption of a Basic Organic Pollutant to a Mineral Surface

Maneerat Ongwandee

Glenn Morrison
Missouri University of Science and Technology, gcm@mst.edu

S. S. Bettinger

Recommended Citation

The influence of ammonia and carbon dioxide on the sorption of a basic organic pollutant to a mineral surface

M. Ongwandee, S. S. Bettinger,G. C. Morrison

University of Missouri-Rolla, Rolla, MO, USA

Abstract

Indoor surfaces have a sorptive capacity for organic pollutants which may be significantly influenced by other gases and the pH of the surface. In this research, we examine the influence of a common indoor gaseous acid, CO_2, and base, NH_3, on the adsorption of a volatile organic base, trimethylamine (TMA), to a mineral surface, zirconium silicate beads. Varying ammonia and carbon dioxide within concentration ranges of indoor relevance substantially influences the sorptive capacity of this mineral surface. Increasing the CO_2 mixing ratio to 1000 ppm enhances surface capacity of TMA by 40 to 50%; increasing the NH_3 mixing ratio to 10 ppm decreases the TMA surface capacity by ~5 to 80% depending on relative humidity. The phenomena of dissolution of TMA into bulk surface water and acid-base chemistry in the surface water do not adequately describe equilibrium adsorption on this surface. Instead, adsorption to the dry solid or to adsorbed water layers appears to dominate. Reduction in the equilibrium partition coefficient, k_e, in the presence of NH_3 is due to a competition between TMA and ammonia molecules for adsorption sites. Site competition appears to follow the Langmuir competitive model and most k_e values range from 0.003 to 0.045 m.

Key words: adsorption, surface chemistry, acidity, organic base, amine, surface characterization

Practical implications
Sorptive interactions with indoor surfaces strongly influence indoor exposure to pollutants. For basic or acidic compounds, these interactions are themselves influenced by surface pH and competition with other acidic or basic gases such as CO_2 and NH_3. We

30 show that CO_2 tends to cause mineral surfaces to store more amines but NH_3 tends to

31 decease this surface capacity. Given the typical range of indoor CO_2 and NH_3

32 concentrations, the indoor reservoir of amines on mineral surfaces may vary by greater

33 than an order of magnitude.

34

35 **1. Introduction**

36   Sorptive interactions are important phenomena that can control indoor air

37 concentrations and occupant exposure. Organic compounds, strongly adsorbed to indoor

38 surfaces, tend to be released over a long time period into indoor air. Familiar examples

39 include odors that linger after cooking or smoking. Indoor surface sorption kinetics and

40 equilibria have been measured by many researchers (e.g. Colombo et al., 1993; Tichenor

41 et al., 1991; Won, 2001), but little is known about the fundamental surface phenomena

42 that control sorption on indoor surfaces. A mechanistic understanding of sorption to real

43 indoor surfaces is an important, but formidable, goal since these surfaces are strikingly

44 complex: mineral and organic, smooth and fleecy/porous, moist and coated with

45 atmospheric deposits, greases and dirt. To initiate this inquiry, a relevant but simple

46 mineral surface was evaluated.

47   Mineral surfaces are common, albeit low capacity, indoor adsorbents and some

48 progress has been made in understanding sorption to these kinds of surfaces. Pennell et

49 al., (1992) found that the vapor sorption of nonpolar organic compounds on hydrated soil

50 and mineral surfaces can be explained as a multimechanistic process including (1)

51 partitioning into organic matter, (2) adsorption on mineral surfaces, (3) dissolution into

52 water films on the surface, and (4) adsorption on surface-bound water. However, the

53 degree of contribution of each process to sorption is dependant on many factors,

54   including relative humidity which can strongly influence the sorptive capacity due to

55   surface site competition or dissolution of polar organic compounds (Goss, 1992).

56   Although researchers have studied the influence of relative humidity (RH) on the

57   sorptive strength of volatile organic compounds (VOCs) on surfaces, it has only recently

58   been recognized that pH and acid-base chemistry at indoor surfaces may be important

59   (Webb, et al. 2002). The surface acidity can vary widely with changing indoor gas-phase

60   concentrations of common indoor acidic and basic compounds such as ammonia, carbon

61   dioxide and vinegar. Webb et al. (2002) studied the influence of ammonia on the

62   adsorption of nicotine on indoor surfaces. They showed that the presence of gas-phase

63   ammonia released by a cleaner can enhance the emission rate of nicotine from a carpet

64   surface. Ammonia somehow modifies the surface, reducing its capacity for nicotine.

65   They inferred that this may be due to an increase in the surface pH, thus driving

66   protonated nicotine to its free-base, volatile form. We suggest that ammonia may instead

67   compete with nicotine for surface sites (e.g. acid sites) and reduce the total surface

68   capacity by taking up available sites.

69   Our broad goal is to develop a better understanding of indoor sorptive phenomena for

70   acidic and basic organic pollutants such as volatile amines and carboxylic acids. The

71   specific objective of this work is to identify surface phenomena governing the strength of

72   sorption of a representative basic organic compound (trimethylamine) to a clean, mineral

73   surface. A variety of surface interactions may contribute to observed adsorption

74   phenomena including direct surface site adsorption and dissolution/acid-base chemistry

75   in bulk surface water. However, to guide our experimental plan, we address two mutually

76   exclusive hypotheses. Hypothesis 1: Aqueous acid-base partitioning of the sorbate

77 effectively stores a substantial amount of the organic base in bulk surface water and

78 controls the overall sorptive capacity; thus the capacity is governed by the aqueous

79 solubility, the pK_a of the sorbate and the pH of bulk surface water. Hypothesis 2:

80 Adsorption of an organic base is primarily a surface phenomenon, i.e. onto the solid

81 surface or onto adsorbed water mono-layers. A decrease in sorptive capacity for an amine

82 in the presence of ammonia is due to competitive adsorption at the surface.

83

84 *1.1 Conceptual model of organic sorption including acid-base chemistry*

85

86 Surface water may act as bulk water at a high relative humidity (RH) on mineral surfaces.

87 Sumner et al. (2004) studied the interaction of water with various surface materials

88 including quartz. Water uptake measurements, using infrared spectroscopy, showed that

89 the surface water film on quartz exhibits spectra similar to bulk liquid water at 80% RH.

90 Thus, overall surface capacity for a sorbate may be mediated by solution chemistry

91 including absorption and acid-base chemistry (right side of Fig. 1). As the relative

92 humidity decreases, disruptions in the hydrogen-bonded network and an increased

93 interaction of the adsorbed water with the surface are observed (Sumner et al., 2004). As

94 the RH decreases, bulk water phenomena should decrease and interactions with a

95 different kind of surface may dominate. At mid-range RH values, several mono-layers of

96 adsorbed water may cover the surface and the species may adsorb preferentially onto the

97 water layer (left side of Fig. 1) (Ong and Lion, 1991; Goss, 1992). At low RH values, the

98 adsorbate will compete with water for dry surface sites.

99

100   *1.2 Hypothesis 1: Dissolution and protonation in bulk surface water controls sorption*

101   We assume here that when the relative humidity is high, bulk water exists on

102   surfaces. The sorptive capacity may then be dominated by dissolution of TMA and

103   protonation in the water film. Given that bulk water is available at high RH, an organic

104   amine is expected to interact with that water according to Henry's law and participate in

105   aqueous acid-base chemistry. Since the aqueous solubility of TMA is large, adsorption at

106   the air-water interface is assumed to be insignificant compared with bulk aqueous

107   phenomena.

108   Thus, gas-phase TMA ($(CH_3)_3N_{(g)}$) partitions to bulk surface water by Henry's

109   law and aqueous TMA ($(CH_3)_3N_{(aq)}$) participates in acid-base equilibrium chemistry:

110

111        $$(CH_3)_3N + H^+ \longleftrightarrow (CH_3)_3NH^+ \tag{1}$$

112

113   At the same time $(CH_3)_3N_{(aq)}$ may physisorb to the surface ($(CH_3)_3N_{(surf)}$) or chemisorb

114   to acidic surface sites ($(CH_3)_3N\text{-}H\text{-}_{(surf)}$) (Boehm et al., 1966). At equilibrium then, the

115   partition coefficient is

116

117    $$k_e = \frac{mass\,of \begin{bmatrix} (CH_3)_3N_{(aq)} + (CH_3)_3NH^+ + \\ (CH_3)_3N_{(surf)} + (CH_3)_3NH-_{(surf)} \end{bmatrix} per\,unit\,surface\,area}{concentration\,of\,(CH_3)_3N_{(g)}} \tag{2}$$

118   The relative influence each form of TMA is uncertain, but all are likely to contribute to

119   the overall adsorptive capacity of the surface.

120   We assume here that k_e is controlled by the two aqueous species of the TMA acid-

121   base equilibrium: neutral and protonated TMA. At a constant gas-phase concentration of

122   TMA, $(CH_3)_3N_{(aq)}$ is assumed to be constant by Henry's law, even if the pH of the water

123   film changes. However, $(CH_3)_3NH^+_{(aq)}$ will increase with decreasing bulk water pH,

124   around the pK_a of TMA. The ratio of neutral to protonated TMA is given by

125

126
$$\frac{\left[(CH_3)_3 N_{(aq)}\right]}{\left[(CH_3)_3 NH^+_{(aq)}\right]} = 10^{(pH - pKa)} \qquad (3)$$

127   As the pH of the bulk surface water increases, as would be the case if the ammonia

128   concentration increases in a room, the fraction of protonated TMA decreases

129   substantially. Therefore, k_e should decrease exponentially over the pH region bracketing

130   the pK_a of the sorbate, and the sorbate will tend to partition to the gas (i.e. be emitted into

131   the room). Defining k_e^o equal to k_e where the pH of a water film is equal to the pK_a, the

132   ratio of k_e/k_e^0 is given by

133
$$\frac{k_e}{k_e^o} = \frac{1 + 10^{(pKa - pH)}}{2} \qquad (4)$$

134   This dimensionless ratio is readily quantified experimentally and should increase

135   exponentially as the pH drops below the pK_a of TMA, if our hypothesis is valid.

136   Otherwise, physisorption and chemisorption to the surface may dominate over dissolution

137   and aqueous protonation.

138   A similar, but not identical, phenomenon may be observed if the surface is

139   covered with acid sites and the amine preferentially chemisorbs to these sites. In this

140   case, the effective surface pK_H may also contribute to an observed increase in k_e as the

141   pH of the bulk water decreases. To address this possibility, we titrated the surface to

142   obtain pK_H and acid site density on the surface (see Methods).

143

144   *1.3 Hypothesis 2: Surface site adsorption controls observed sorption.*

145

146   Instead of dissolving into bulk surface water, an amine adheres to the surface,

147   either by chemisorption or physisorption to dry surface sites or to adsorbed water. As a

148   result, any influence of CO_2 or NH_3 on TMA adsorption is due to modification of the

149   surface itself. We approach this hypothesis by testing two related phenomena:

150   competitive adsorption (NH_3 and TMA) and isotherm analysis.

151   Active competition for surface sites may explain why ammonia influences surface

152   capacity. Competitive adsorption is well characterized by Langmuir (Weber, Jr and

153   DiGiano, 1996). The Langmuir isotherm, one of several well known adsorption models,

154   has been developed on the basis of dynamic equilibrium (Thomas and Crittenden, 1998).

155   The isotherm assumes that adsorption occurs in one molecular layer of a sorbate on the

156   surface with no interaction between sorbate molecules. Moreover, adsorption energy is

157   assumed to be constant, i.e., the surface sites are homogenous. If multiple sorbate species

158   are present and the concentrations are high enough for the isotherm to exhibit non-

159   linearity, the sorbates may compete for sites and disrupt their respective adsorption

160   capacities. To apply an isotherm model which includes the effect of competition to

161   experimental data, the model should be able to describe the adsorption of each compound

162   over the concentration range of interest. Therefore, the Langmuir equation can be

163   modified to predict the competitive adsorption among sorbates, where each sorbate

164   independently follows the Langmuir isotherm. The Langmuir competitive adsorption, $q_{e,i}$

165   of the ith sorbate from an *n*-sorbate mixture is given by (Weber, Jr and Digiano, 1996)

$$q_{e,i} = Q^o_{a,i} b_i C_{e,i} \left(1 + \sum_{j=1}^{n} b_j C_{e,j} \right)^{-1}$$

166 (5)

167

168   q_e = amount of sorbate adsorbed per unit area of sorbent at equilibrium ($\mu g\ m^{-2}$)

169   Q^o_a = maximum adsorption capacity ($\mu g\ m^{-2}$)

170   b = coefficient related to the net enthalpy of adsorption ($m^3\ \mu g^{-1}$)

171   C_e = sorbate concentration at equilibrium ($\mu g\ m^{-3}$)

172

173   A substantial increase in the gas-phase concentration of any species j will decrease the

174   surface capacity of competing species i. Thus, hypothetically, an increase in ammonia

175   from using a cleaner decreased the surface capacity of nicotine on the carpet in Webb et

176   al. (2002).

177   In testing this hypothesis, the effect of pH must be isolated. For example,

178   increasing the gas-phase concentration of ammonia may indeed displace TMA, but it will

179   also increase pH. By combining NH_3 and CO_2, the pH can be controlled. Any pH

180   independent displacement of TMA is due to surface phenomena because NH_3 will not

181   displace TMA in bulk water at a constant pH and temperature. Thus TMA sorption is a

182   solid-surface phenomenon if we observe 1) pH independent displacement of TMA, and

183   2) predictive Langmuir competitive adsorption behavior.

184

185   **2. Methods**

186

187   *2.1 Materials*

188

189   The sorbent chosen was zirconium silicate in the form of 0.18 cm diameter beads

190   (Ceroglass, Inc.). This glassy surface is representative of indoor materials such as

191   window glass, or more porous mineral furnishings such as granite countertops, aggregate

192   in concrete or mineral fibers in ceiling tiles. The beads were sonicated in

193   distilled/deionized water for 30 minutes to remove impurities, and then baked in an oven

194   at 60ºC for at least 6 hours prior to experimentation.

195   The sorbate chosen was trimethylamine (TMA). TMA is mildly basic with a pK_a of

196   9.8 and is functionally similar to nicotine with a pK_2 of 8.0 (Pankow et al., 1997). It is

197   more volatile and less toxic than nicotine, and easier to work with in experiments. TMA

198   is also an important odorous air pollutant of indoor interest in its own right. It is

199   commonly encountered as a nuisance odor from livestock operations (O'Neill and

200   Phillips, 1992). At a pK_a of 9.8, significant changes in acid-base aqueous partitioning

201   may occur in bulk surface water at realistic indoor ammonia concentrations.

202

203   *2.2 Experimental apparatus*

204

205   The evaluation of indoor surface sorption parameters is typically performed in a

206   Continuously Mixed Flow Reactor (CMFR) style chamber (Won et al., 2001). These

207   chambers provide environmental conditions and near-surface velocities that are

208   comparable with those found indoors. However, the sorptive capacity of glassy surfaces

209   is often at or below detection limits when measured in this configuration. To improve our

210   ability to quantify sorptive capacity and distinguish among surface phenomena, we chose

9

211 to measure the equilibrium partitioning in a Plug Flow Reactor (PFR). This configuration

212 allows us to increase the total silicate surface area in the reactor, increasing total adsorbed

213 mass and reducing uncertainty in the measurements.

214   Shown in Fig. 2 is a diagram of the experimental apparatus. The core component is a

215 50 cm Teflon reactor with an inner diameter of 1.8 cm for measuring sorption equilibria.

216 The reactor is completely filled with zirconium silicate beads. TMA and water are

217 simultaneously introduced into the system using a syringe pump. The solution is

218 evaporated and diluted with high purity nitrogen (flow path A). The syringe pump

219 delivers an aqueous TMA solution at a rate calculated to achieve a desired gas-phase

220 concentration and relative humidity (RH) at a total gas flow of 500 ml min^{-1}. For example

221 a 630 mg l^{-1} solution of TMA in water delivered at a volumetric flowrate of 0.38 ml hr^{-1}

222 and diluted with nitrogen gas generates a gas-phase mixing ratio of 3 ppm TMA at 50%

223 RH and a total gas flow of 500 ml min^{-1}. Heat tape is wrapped around the tubing at the

224 point of injection to help evaporate the TMA solution into the system. Humidified

225 nitrogen is delivered in a similar fashion in a separate gas line except that deionized (DI)

226 water was used instead of a TMA solution (flow path B). To adjust the pH of the aqueous

227 surface film, gas-phase ammonia and carbon dioxide are delivered via a 3-way Teflon

228 solenoid valve to the total gas flow to achieve a desired pure-water equilibrium pH by

229 Henry's law (Nazaroff and Alvarez-Cohen, 2001). The outlet gas is split into two

230 streams: 50 and 450 ml min^{-1}. The 450 ml min^{-1} stream is delivered to a flask where pH,

231 temperature, and RH are measured. We confirm the predicted pH of bulk surface water

232 by sparging the exhaust air through 2-ml DI water via a gas dispersion frit (Ace Glass,

233 Inc.) and measuring the pH of that water using a pH probe. Note that the *reported* pH is

234 calculated based on Henry's law and acid-base equilibria; the primary purpose of the pH

235 measurement is to ensure that the experimental system is working properly. Due to small

236 losses in the system, an actual flow of 40 ml/min is delivered to a continuous analyzer for

237 quantification. All experiments are conducted at 25ºC and the internal pressure of the

238 Teflon reactor is 1.1 atm.

239   For experiments conducted at a gas-phase mixing ratio ≥ 1 ppm TMA, we use a flame

240 ionization detector (FID) with a detector temperature of 250ºC. For experiments

241 conducted at 50 and 100 ppb, a chemical ionization mass spectrometer (CIMS) is used. In

242 our CIMS system, we employ a proton transfer reaction using protonated water as a

243 reagent ion to ionize TMA molecules (Španěl and Smith, 1998). Protonated TMA is then

244 detected by a quadruple mass spectrometer (ABB Extrel, Inc.). The FID and pH meter are

245 connected to a data acquisition system in which the data were directly stored in the

246 computer, while the temperature and RH were recorded manually.

247   For ammonia sorption experiments, we use a sample-draw transmitter (Thermo Gas

248 Tech, Inc.) to detect and quantify ammonia. The instrument has its own pump and

249 requires an air flow rate of 280 ml min^{-1}. The remaining flow is directed to a flask where

250 pH, RH, and temperature are measured.

251

252 *2.3 Experimental procedures*

253

254   Clean humidified nitrogen (flow path B) is first supplied to the reactor until the

255 desired RH, measured at the exhaust, is reached. Subsequently, a sorption stage is

256 initiated by introducing gas-phase TMA to the reactor (flow path A) while at the same

257 time directing the clean humidified nitrogen to a vent. This stage typically requires

258 approximately one hour to achieve equilibrium but is allowed to run for an additional 30

259 minutes to obtain an average signal value for gas calibration. The humidified nitrogen is

260 then redirected to the reactor (flow path B) while the gas-phase TMA is redirected to a

261 vent. This desorption stage also requires about one hour. The k_e value is determined from

262 total mass of TMA accumulated per unit surface area divided by inlet sorbate

263 concentration. By convention for indoor materials, k_e is referenced to the geometric

264 surface area, not the total surface area (i.e. internal pore area). To quantify the total mass

265 accumulated, we apply the trapezoid rule to calculate the sorption area which excludes

266 the pre-determined lag time of the system and we then convert this sorption area to mass

267 using a two-point calibration on either the FID or CIMS as appropriate. The reactor lag

268 time was determined by performing a pulse residence time distribution using propane as a

269 conservative tracer.

270   The isotherm experiments were conducted at 20, 50, and 90% RH and at five

271 different TMA inlet mixing ratios of 0.1, 1, 2, 3, and 6 ppm. At 50% RH, 50 ppb TMA

272 was additionally studied. To determine the influence of the surface pH on k_e values, the

273 experiments were conducted at three relative humidity conditions but only 3-ppm TMA

274 was used. Ammonia and carbon dioxide gases were added at the inlet flow to obtain a

275 desired pure-water equilibrium pH, varying from 8 to 11 which covered a pH region

276 around a TMA pK_a of 9.81.

277   To test the hypothesis that ammonia displaces TMA at surface sites, regardless of the

278 water-film pH, we performed two experiments at the identical pH value. In the first, only

279 TMA was present (from an isotherm experiment). In the second, TMA, NH_3 and CO_2

280   were all present but the inferred surface water-film pH (pH=9.6) was the same as for the

281   previous experiment. We conducted a sorption experiment at 50% RH and TMA mixing

282   ratio of 3 ppm by adding gas-phase ammonia at 800 ppm to the total flow. Carbon

283   dioxide at 200 ppm was also added to maintain the pH of the water film constant to

284   ensure that the influence of ammonia on k_e was independent of a change of the pH. Clean

285   humidified nitrogen along with ammonia and carbon dioxide were initially supplied to

286   the reactor until the relative humidity reached 50%, then gas-phase TMA was introduced.

287

288   *2.4 Quantification of surface acid sites, surface area and pore distribution*

289

290   To better understand the sorptive behavior of TMA, we have further studied the

291   surface physical/chemical characteristics of the zirconium silicate beads used in this

292   work. The acid site density, Γ_m, (mol/g of solid) and acidity constant, pK_H, of the surface

293   were determined using a batch equilibrium acidimetric-alkaline titration method

294   developed by Wang et al. (2000). We used a solid to liquid ratio of 50 g of beads to 100

295   ml of 0.01 M $NaNO_3$ solution. Accessible surface area and pore volume distribution were

296   determined using N_2 BET and BJH desorption analyses.

297

298   *2.5 Bulk water equilibrium pH in contact with residential air*

299

300   Since bulk water surface pH is an important variable in this study, we measured the pH of

301   purified water in contact with air in residences. We sought to 1) obtain "typical values"

302   and 2) determine if the measured levels of indoor CO_2 and NH_3 are sufficient to predict

303   bulk water pH. We measured the pH using a method similar to that used in the sorption

304   experiment. A sampling pump (MSA Co.) was used to draw ambient air at a rate of 2 l

305   min^{-1} through 25-ml de-ionized water. A pH probe was installed in the water and the pH

306   was measured at 5 minute intervals for 30 minutes. We report the final pH values here.

307   While measuring the pH, we also measured the concentrations of ammonia and carbon

308   dioxide as well as the relative humidity using a photo-acoustic multi-gas monitor (Brüel

309   & Kjær, Inc.). One set of pH measurements was conducted in a kitchen while a

310   commercial liquid ammonia (~10%) cleaner was applied to the floor. The occupant

311   washed the kitchen floor using a sponge soaked with ammonia cleaner for 20 minutes.

312   The experiment was carried out in residence occupied by 2 people, 2 dogs and 1 cat.

313

314   **3. Results**

315

316   *3.1 Bulk water pH, TMA pK$_a$ and dissolution do not explain adsorption behavior*

317   Fig. 3 shows anticipated and experimental responses of k_e as the pH of hypothetical

318   bulk surface water is modified by adding either gas-phase ammonia or carbon dioxide. In

319   this figure, the partition coefficient is normalized by the value measured at pH = 9.8 (the

320   pK$_a$ of TMA). The model curve was derived from Eq. (3). The experimental results

321   shown were carried out at 90% RH to ensure that some bulk surface water is present.

322   If only aqueous chemistry in the bulk surface water influences overall adsorption, the

323   model predicts a substantial increase in the ratio of k_e/k_e^o as the pH decreases. However,

324   this ratio only increases modestly as the pH of bulk water on the surface is decreased by

325   contacting the surface with carbon dioxide at 28 and 1000 ppm, corresponding to water

14

326   pH of 8.8 and 8.0 respectively. We note that an inflection point occurs between pH 9.6

327   and 10. This occurs at about the pK_a of TMA, but also occurs where ammonia is added to

328   raise the pH.

329

330   *3.2 RH, CO_2, and NH_3 influence partition coefficient*

331

332   Fig. 4 shows the relationship between k_e and relative humidity at various inlet mixing

333   ratios. The decline of the k_e values with increasing the relative humidity or the amount of

334   surface water is observed at all inlet mixing ratios, especially at a lowest mixing ratio of

335   0.1 ppm. The results for TMA at 0.1 ppm exhibits unusual behavior as the k_e value at

336   20% RH is reproducibly much higher (0.22 m) than anticipated given trends for 2 ppm

337   TMA and greater. A similar, but more modest, inflection is observed for the 1 ppm

338   results, where the partition coefficient at 20% RH is somewhat higher than would be

339   anticipated given the results at higher TMA mixing ratios.

340   Carbon dioxide and ammonia appear to significantly modify the adsorptive surface

341   capacity for TMA as shown in Figure 5. For CO_2 an increase in k_e values was observed

342   for all RH values from dry to humid. Even a modest mixing ratio (28 ppm) of CO_2

343   appears to enhance the sorption coefficient at all tested RH values. At a realistic CO_2

344   mixing ratio (1000 ppm), we observe a moderate increase in the surface capacity for

345   TMA at all RH values. At 90% RH, where bulk surface water may reasonably be

346   assumed to exist, CO_2 has the effect of increasing the surface capacity for TMA by

347   ~60%. For a modest mixing ratio of NH_3 (10 ppm), the TMA capacity decreases a small

348   amount at low RH, but k_e decreases by a factor of 2 and 6 at 50% and 90% RH

349   respectively. At a very high mixing ratio of NH$_3$ (1000 ppm) the surface capacity for

350   TMA is almost completely depleted and k_e is reduced by a factor of 8 to 20.

351

352   *3.3 TMA follows Langmuir isotherm and competitive adsorption with NH$_3$ is observed*

353

354   To explore the possibility that amines preferentially sorb to the solid surface (instead

355   of bulk surface water), we evaluated the surface capacity over a wide range of gas

356   concentrations. We also evaluated the equilibrium adsorption behavior of ammonia. For

357   both species, we observe nonlinear sorption isotherms as illustrated in Fig. 6. At each RH

358   value, the isotherm appears to follow the Langmuir model, where sorptive capacity

359   decreases at higher concentrations because fewer surface sites are available for sorption.

360   At the highest TMA concentration, we observe a distinct increase in capacity that

361   deviates from the Langmuir model. The single-sorbate isotherms of TMA at 20, 50, and

362   90% RH along with ammonia at 50% are fit to the Langmuir isotherm with R^2 equal to

363   0.97, 0.99, 0.95, and 0.91 respectively. Table 1 shows the Langmuir constants (from Eq

364   (5)), Q_a^0, and b, and k_e values obtained from a multiple of Q_a^0 and b.

365   To develop a competitive adsorption model, we apply the Langmuir-type competitive

366   model (Eq (5)) to experimental observations of pure species isotherms, since each

367   gaseous compound (TMA and ammonia) exhibits Langmuir isotherms up to a gas phase

368   TMA mixing ratio of 3 ppm (Fig. 6). Calibrating with isotherm parameters derived from

369   pure species isotherms (Table 1, 50% RH), we should be able to predict the surface

370   capacity for TMA in the presence of NH$_3$ if the competitive hypothesis is correct. To

371   verify the model, we conducted TMA sorption experiments at 3 ppm with ammonia

372   mixing ratios of 10, 20, and 40 ppm. The experiments were also conducted at 50% RH.

373   As shown in Fig. 7, the calibrated model adequately describes TMA adsorption

374   influenced by gas-phase ammonia at 50% RH.

375   To demonstrate that ammonia competes with TMA for surface sites in the absence of

376   pH change, the equilibrium surface capacity was determined for two different ammonia

377   concentration levels as described in the Methods section. Recall that CO_2 was used to

378   ensure that any bulk water remained at the same pH (9.6). The 50% RH isotherm for

379   TMA, in the absence of NH_3, is reproduced in Fig. 8. This isotherm can then be

380   compared with a set of results obtained at an ammonia mixing ratio of 800 ppm. The

381   equilibrium capacity of TMA sorbed on the surface was decreased by a factor of 40 in the

382   presence of ammonia. This pH-independent decrease in capacity suggests that ammonia

383   and TMA are competing for surface sites.

384

385   *3.4 Surface acid site characterization*

386

387   Fig. 9 shows the result of a net titration for the zirconium silicate beads using the

388   method of Wang et al. (2000). The surface contains three types of acid sites. Their pK_H

389   are 2.5, 6.5, and 11.0 with the surface sites per unit area of 1.8×10^{-5}, 2.4×10^{-6}, and 6.3

390    $\times 10^{-6}$ mol m^{-2}, respectively (based on N_2 BET surface area). Surface area accessible to

391   N_2 by BET analysis was 0.16 m^2 g^{-1}, roughly 300 times greater than the superficial area

392   of the beads of 0.00054 m^2 g^{-1}.

393

394   *3.5 Bulk water equilibrium pH ~5.2 in contact with residential air*

395

396   Table 2 shows the final pH values, mean values of mixing ratios of carbon dioxide

397   and ammonia, and RH measured in five residences between 11/22/04 and 12/05/04.

398   These compare well with reported range of residential ammonia and carbon dioxide

399   mixing ratios of 1-60 ppb (Brauer et al., 1991, Atkins and Lee, 1993; Suh et al., 1994)

400   and 300-3500 (Seppänen et al., 1999) respectively. The measured pH values in this study

401   range from 5.0 to 5.2 which are somewhat lower than the predicted values determined on

402   the basis of Henry's law and acidity constants of carbon dioxide and ammonia gases.

403   This may be because of the presence of other acidic gases (Brauer et al., 1991) that could

404   lower the pH such as nitric acid, carboxylic acids etc. In these apartments, the carbon

405   dioxide concentrations were at about the anticipated level for modest ventilation rates

406   during winter.

407   We also measured the equilibrium water pH while the occupant washed the kitchen

408   floor with an ammonia cleaner. The measured pH and ammonia mixing ratio are shown

409   in Fig. 10. The average mixing ratio of carbon dioxide was 840 ppm and relative

410   humidity was 52% during the experiment. As the ammonia cleaner (pure solution from

411   the bottle) was introduced, the ammonia mixing ratio increased to 46 ppm and the pH

412   increased to 8.5, which is in agreement with the predicted value of 8.7. With time, the

413   ammonia concentration decreases by ventilation, and perhaps deposition, and the pH

414   decreases.

415   **4. Discussion**

416   Broadly, our results point away from hypothesis 1 (bulk surface water and solution

417   chemistry) and towards hypothesis 2 (surface interactions). Several lines of evidence

18

418   argue against bulk water chemistry driving sorption. However, some observations suggest

419   that acid-base chemistry in bulk water contributes in a modest way to the overall surface

420   capacity for trimethylamine.

421   *4.1 Evidence against bulk water chemistry controlling adsorption*

422   The first indication that bulk water chemistry is less important in sorption is that the

423   sorption behavior as pH changes does not match model behavior predicted by hypothesis

424   1 as shown in Fig.3. Instead of an exponential decrease in surface capacity as pH

425   increases, we observe an inverted S-shaped curve with a strong inflection at the point

426   where ammonia is introduced. This poor fit of the experimental results from the predicted

427   model suggests that a change of surface water film pH is not a key parameter that governs

428   the vapor sorption of TMA on the hydrated zirconium silicate surface.

429   Further evidence against hypothesis 1 comes from the relative humidity results. The

430   TMA surface capacity is observed to decrease in Fig. 4 at all TMA mixing ratios as RH

431   increases. Given that Sumner et al. (2004) found that bulk water exists above 80% RH on

432   mineral surfaces, we would anticipate that increasing RH from 50% to 90% RH will

433   result in a significant increase in the total volume of bulk water on the surface. In this

434   case, more water means more TMA adsorption capacity by dissolution. Instead, we

435   observe a decrease in overall surface capacity for TMA at RH increases.

436

437   *4.2 Evidence for solid surface/hydrated surface adsorption*

438

439   Solid-surface or air-water interfacial interactions appear to overwhelm any increase in

440   TMA absorption/dissolution capacity in the bulk water. Sumner et al. (2004)

441   characterized the hydrated glass surface using atomic force microscopy and found that

442   water does not completely cover the surfaces even at RH above 60%. Instead, the

443   surfaces are covered with water islands. However, the relationship between the fraction

444   of the surfaces covered with such water islands and the relative humidity was not studied,

445   only equivalent number of water monolayers were reported. Therefore, at moderate to

446   high RH conditions, TMA may simultaneously be bonded to dry surface, adsorbed water

447   molecules and dissolved into bulk water.

448   Our humidity-dependent adsorption results echo those of Goss (1992). Goss studied the

449   sorptive capacity of 17 polar and non-polar organic compounds on quartz sand at RH

450   ranging from 10 to 90%. Goss found that k_e values decrease with increasing RH. Below

451   26% RH, equivalent to one molecular layer of adsorbed water, adsorption of organic

452   molecules on free water surface sites is an important sorption mechanism, while

453   adsorption on the surface coated by a complete water film becomes dominant as the RH

454   increases above 26%. Goss also suggested that competitive adsorption between organic

455   and water molecules contributes to a decrease in k_e in the RH region below 26% since

456   water molecules are preferentially adsorbed on the mineral surface. In addition, the Goss

457   study of heats of sorptions at 30-70% RH showed that the polar sorbents containing

458   oxygen atoms have higher heats of sorptions than their heats of condensation. This was

459   explained by an increase in binding forces between the hydrogen of the water and the

460   electron donors of the sorbates at the liquid –gas interface. Thus, instead of competition

461   for dry surface sites between TMA and water, we may be observing progressively weaker

462   binding of TMA to sorbed water molecules as the number of monolayers increases with

463   RH.

464   Similar behavior was observed in a study of gas-phase trichloroethylene (TCE) sorption

465   to soil minerals. Based on their results, Ong and Lion (1991) proposed sorption processes

466   corresponding to three regions. 1) Below one monolayer of adsorbed water, the

467   observations based on heats of sorption were similar to Goss' (1992) study. Direct vapor

468   adsorption on the solid surface and competition with water molecules were indicated. 2)

469   Between one and five layers of water coverage, the sorption was attributed to adsorption

470   of trichloroethylene onto surface-bound water rather than dissolution into adsorbed water.

471   The dissolution limitation may be due to a modification of the first several layers of

472   adsorbed water by interaction with the mineral surface. Ong and Lion did not observe

473   competition between water and sorbate molecules for sorption in this region. We may

474   tentatively conclude that TMA competition with water molecules for dry surface sites at

475   50% RH contributes to sorption in a minor way. 3) Above five layers of adsorbed water,

476   dissolution of TCE into condensed water and partitioning at the solid-liquid interface

477   become dominant.

478   Considering these findings and our results, dissolution into adsorbed bulk water is

479   probably not the major contributor to the sorption of TMA even at 90% RH where

480   surface water is expected to behave like bulk water. However, without experimental

481   results at 0% RH, we may not conclude that adsorption on the water-free surface is the

482   dominant sorption mechanism. At low humidity and low TMA concentrations, we

483   observed that $ZrSiO_2$ surface had an unusually high capacity for TMA (Fig. 4). Goss

484   (1992) also observed unusually high k_e values for organics on mineral surfaces at

485   humidities below 26%. It is unclear why this phenomenon was not observed for TMA at

486   mixing ratios >1 ppm. However, this suggests that measurements of sorption

487 characteristics for polar, acidic or basic compounds should continue to be carried out at

488 mixing ratios relevant to indoor conditions, e.g., in the ppb range for most organics.

489

490 *4.3 CO_2 and NH_3 modify the adsorptive surface capacity for TMA*

491

492 While we conclude that aqueous chemistry in bulk water is not the major contributor to

493 sorbent capacity, we do observe phenomena that point to acidification of either the dry

494 solid surface, surface bound water or bulk water. Fig. 5 demonstrates that CO_2 tends to

495 increase the sorbent capacity of TMA at all RH. Comparing the trends in k_e (Fig. 4 and

496 Fig. 5) as RH increases, we observe that CO_2 has the effect of offsetting the water

497 induced reduction in TMA capacity. At 20 and 50% RH, an increase in k_e may be

498 explained by an acidification of the surface-bound water by carbon dioxide, thus

499 increasing the acidic sites for TMA molecules to be adsorbed onto. At 90% RH, an

500 increase in k_e may also be due to an increase in protonated TMA as the adsorbed bulk

501 water has become more acidic. In addition, TMA dissolved in the bulk water could

502 chemisorb onto solid surface sites made increasingly acidic by carbon dioxide.

503 Conversely, NH_3 may deplete acid sites. The depleting influence of NH_3 appears to be

504 enhanced by increasing relative humidity, possibly indicating that aqueous phenomena

505 are still important.

506 As shown in Fig. 3, an inflection point occurs as gas-phase ammonia is used to increase

507 the pH of the water film. Since we have concluded that dissolution of TMA into bulk

508 liquid water on the surface is not the key sorption mechanism, we hypothesize that the

509 significant reduction in the surface capacity for TMA is attributed to a competition

510   between TMA and ammonia molecules for surface sites. The isotherm measurements

511   shown in Fig. 6 are clearly non-linear and appear to fit the Langmuir model (see Table 1).

512   Combining independently derived Langmuir coefficients we show in Fig. 7 that the

513   reduction in the partition coefficient, in the presence of ammonia, is predictable.

514   Combined, these results point strongly to surface sorption (either dry or adsorbed water)

515   with competition for sites between TMA and NH_3. Even if the hypothetical surface water

516   pH is held constant, we show in Fig. 8 that NH_3 clearly displaces TMA. We note that the

517   sorbent capacity results at a high TMA concentration appear to deviate from the

518   Langmuir model. This is probably due to the formation of multiple layers of TMA at the

519   high relative pressure of the sorbate.

520   Our analyses of surface acid sites yields some clues about sorption mechanisms. We

521   determined surface pK_a values at 2.5, 6.5 and 11. At these pK_a values we would

522   anticipate a significant shift in surface acid site density. Within our design pH range (8 to

523   11) of bulk surface water, we would anticipate a change in available acid sites by about a

524   factor of two. If chemisorption is an important mechanism, this could explain some of the

525   decrease in surface capacity as pH increases. Since NH_3 appears to participate in

526   competitive adsorption with TMA, the pH range between 8 and 9.6 is more useful. In this

527   range, only CO_2 is used to adjust acidity. From pH 8 to 9.6, surface acid site density

528   should decrease by about 14%. This may contribute to a portion of the observed 40%

529   increase in TMA capacity. A caveat: given that the nature of the water on the surface is

530   unknown, applying the concept of pH the bound surface water may be unrealistic.

531

532   *4.4 Solid surface acid sites account for small fraction of TMA capacity*

533

534   Acid site density is consistent with surface area measurements, but not with TMA

535   coverage. The acid sites with $pK_H = 11$ are of interest in this research since we have

536   studied the influence of the surface pH ranging between 8 and 11. Based on BET surface

537   area measurements, the surface concentration of acid sites is 6.3×10^{-6} mol m^{-2},

538   corresponding to a site area of 2.6×10^{-15} cm^2 site^{-1}. This corresponds to a reasonable site

539   diameter of roughly 5 Å. The highest predicted TMA coverage based on isotherms is

540   much smaller than anticipated if driven primarily by density of acid sites. Given a density

541   of liquid TMA of 0.657 g cm^{-3} (Matheson Co., 1961), the cross-sectional area of one

542   TMA molecule is 3.4×10^{-15} cm^2 (or 4.9×10^{-6} mol m^{-2}). This area closely corresponds to

543   the acid site area. However, the maximum adsorption capacity at 20% RH ($\sim 1.1 \times 10^{-8}$

544   mol m^{-2}) is only small fraction of the measured acid site density. Interestingly, surface

545   coverage of TMA at low humidity corresponds more closely to the superficial geometric

546   surface area of the beads. Pore size distribution analysis showed that most pores are 20 Å

547   or greater in diameter and that most internal porosity should be available to TMA.

548

549   *4.5 Partition coefficient smaller than that observed for other indoor surface-organic*

550   *interactions*

551

552   The k_e values obtained for our glassy surface (mostly lying between 0.003 and 0.04 m)

553   are somewhat higher than that reported by Goss (1992) for a variety of polar and non-

554   polar organic species on quartz (ranging from 10^{-6} to 10^{-4} m). Referencing our k_e results

555   to the BET surface area ($k_{e,BET}$ ranges from 10^{-5} to 10^{-4} m) instead of the geometric area

556   results in a better correspondence with Goss. Our results are much lower than values

557   reported by other researchers which typically lie between 0.1 and 5 m for indoor surfaces

558   (Won, 2001; Tichenor et al., 1991). Unfortunately, indoor surface researchers were

559   unable to quantify k_e on glass due to low sorption strength and limitations of their

560   equipment (Tichenor et al., 1991). The closest material for comparison would be ceiling

561   tiles which are composed of mineral fibers. The values reported are about 5-10 times

562   greater for TCE than our values for TMA. However, the basis of k_e is the superficial

563   planar area of the ceiling tile while our values are based on the "true" surface area of the

564   beads. Furthermore, ceiling tiles are often painted and TMA was not tested as a sorbate.

565   For these reasons, we find it difficult to compare our k_e values with those determined on

566   other indoor materials.

567   **5. Conclusions**

568   These experiments demonstrate that dissolution into bulk surface water along with

569   acid-base chemistry on the surface is not the major sorption process for a representative

570   amine on a mineral surface. However, carbon dioxide contributes to a modest increase in

571   k_e. Carbon dioxide may acidify the surface-bound water, thereby increasing the number

572   of available acid sites. Unlike the influence of carbon dioxide on k_e, gas-phase ammonia

573   reduces the sorptive strength substantially. This phenomenon is explained by a

574   competition between ammonia and TMA molecules for adsorption sites. The adsorption

575   isotherms reasonably fit the Langmuir competitive model.

576   Development of equilibrium adsorption isotherms and kinetic parameters in the

577   absence of the appropriate levels of sorbate, water, CO_2 or NH_3 can lead to unreliable

578   results. Other acidic or basic gases and aerosols are present indoors (Brauer et al., 1991)

579 and may also become important in understanding adsorption. Non-linear sorption for

580 TMA at levels as low as 1 ppm suggests that future research on the sorption of similar

581 species cannot rely on an assumed linear isotherm. Because of the difficulty in detecting

582 species such as TMA and nicotine, researchers may be tempted to use high

583 concentrations for convenience. However, adsorption isotherms representative of indoor

584 TMA concentrations must be performed at gas-phase concentrations significantly less

585 than 1 ppm, and preferably in the appropriate range for that species in typical indoor

586 settings. To our knowledge, this is the first example of enhanced sorptive capacity of

587 indoor materials due to CO_2. Because of its ubiquity and variability in indoor

588 environments, it is especially important for future adsorption research on acidic or basic

589 compounds to include CO_2 in the diluent gas.

590   In considering the impact these findings have on understanding indoor air quality, we

591 recognize that glassy surfaces are generally low-capacity sorbents unlike carpet or

592 painted walls. However, this research should help guide research on more complex

593 indoor surfaces. For example, if bulk water exists on painted wall board at moderate to

594 high RH, then the capacity for basic compounds should increase with increasing CO_2.

595 Given the functional similarity between ammonia and organic amines, we anticipate that

596 these compounds will participate in competitive adsorption if suitable acidic surface sites

597 exist, regardless of surface.

598 As typified by our residential experiments and prior research (Brauer et al., 1991; Atkins

599 and Lee, 1993; Seppänen et al, 1999), "normal" indoor conditions roughly correspond to

600 mixing ratios for CO_2 and NH_3 of >500 and < 0.2 ppm respectively. Generally, we would

601 expect amine and ammonia levels to be low enough that their respective adsorption

602   isotherms will fall in the linear range. Therefore, competitive adsorption should not be a

603   major factor influencing surface capacity. In this case, any pH driven changes (e.g. by

604   CO_2) may indeed become more important, in a relative sense. However, sharp increases

605   in ammonia from cleaning (Fig.10) or from animal/human wastes are common and

606   clearly increase the NH_3 concentration into a non-linear adsorption regime. These events

607   are certain to drive amines off mineral surfaces, by the mechanism of competitive

608   adsorption, and into the breathing zone. Considering Webb et al. (2002) results in this

609   light, the pH change due to an ammonia cleaning episode is more than enough to shift the

610   acid-base partitioning of nicotine ($pK_a = 8$) in a water film, but is not sufficient to shift

611   the acid-base partitioning of TMA ($pK_a = 9.8$). Competitive adsorption may also explain

612   the observation that nicotine desorbs rapidly in the presence of ammonia. Yet, structural

613   differences between TMA and nicotine, and differences among surfaces tested make any

614   conclusive comparisons between these systems premature.

615   The next steps are clear. We must evaluate the adsorption equilibria and kinetics for

616   the more complex surfaces that are so ubiquitous in indoor environments such as carpet

617   and paint. In addition, we need to expand the suite of sorbates to include other amines

618   and acids. We have begun evaluating these equilibrium phenomena with painted surfaces.

619   However, we are finding that paint exhibits behavior that is very different from the

620   zirconium silicate beads. Therefore, we emphasize that the results from the present

621   research is relevant to mineral surfaces only.

630
631   **References**
632
633   Atkins, D.H.F., Lee, D.S. (1993) "Indoor concentrations of ammonia and the potential
634   contribution of humans to atmospheric budgets", *Atmospheric Environment*, **27A**, 1-7.
635
636   Boehm, H. P. (1966) in *Advances in Catalysis and Related Subjects*, Eley, D. D., Pines,
637   H., and Weisz, P. B., eds, New York, Academic Press.
638
639   Brauer, M., Koutrakis, P., Keeler, G.J., Spengler, J.D. (1991) "Indoor and outdoor
640   concentrations of inorganic acidic aerosols and gases", **41**, 171-181.
641
642   Colombo, A., De Bortoli, M., Knöppel, H., Pecchio, E., and Vissers, H. (1993)
643   "Adsorption of selected volatile organic compounds on a carpet, a wall coating, and a
644   gypsum board in a test chamber", *Indoor Air*, **3**, 276-282.
645
646   Goss, K. (1992) "Effects of temperature and relative humidity on the sorption of organic
647   vapors on quartz sand", *Environmental Science and Technology*, **26**, 2287-2294.
648
649   Matheson Company Inc. (1961) *Matheson Gas Data Book*. East Rutherford, N.J.
650
651   Nazaroff, W. W., and Alvarez-Cohen, L. (2001) *Environmental Engineering Science*,
652   New York, John Wiley & Sons, Inc.
653
654   O' Neill, D. H., and Phillips, V. R. (1992) "A review of the control of odor nuisance from
655   livestock buildings: Part 3, properties of the odorous substances which have been
656   identified in livestock wastes or in the air around them", *Journal of Agricultural
657   Engineering Research*, **53**, 23-50.
658
659   Ong, S. K., and Lion, L. W. (1991) "Mechanisms for trichloroethylene vapor sorption
660   onto soil minerals", *Journal of Environmental Quality*, 20, 180-188.
661
662   Pankow, J. F., Mader, B. T., Isabelle, L. M., Luo, W., Pavlick, A., and Liang, C. (1997)
663   "Conversion of nicotine in tobacco smoke to its volatile and available free-base form
664   through the action of gaseous ammonia", *Environmental Science and Technology*, **31**,
665   2428-2433.

666
667 Pennell, K. D., Rhue, R. D., Rao, P. S. C., and Johnston, C. T. (1992) "Vapor-phase
668 sorption of *p*-xylene and water on soils and clay minerals", *Environmental Science and*
669 *Technology*, **26**, 756-763.
670
671 Seppänen, O.A., Fisk, W.J., Mendell, M.J. (1999) "Association of ventilation rates and
672 CO_2 concentrations with health and other responses in commercial and institutional
673 buildings", *Indoor Air*, **9**, 226-252.
674
675 Španěl, P., and Smith, D. (1998) "Selected ion flow tube studies of the reactions of H_3O^+,
676 NO^+ and O_2^+ with several amines and some other nitrogen-containing molecules".
677 *International Journal of Mass Spectrometry*, **176**, 203-211.
678
679 Suh, H.H., Koutrakis, P., Spengler, J.D. "The relationship between airborne acidity and
680 ammonia in indoor environments". *Journal of Exposure Analysis and Environmental*
681 *Epidemiology*. **4**, 1-23.
682
683 Sumner, A. L., Menke, E. J., Dubowski, Y., Newberg, J. T., Penner, R. M., Hemminger,
684 J. C., Winger, L. M., Brauers, T., and Finlayson-Pitts, B. J. (2004) "The nature of water
685 on surfaces of laboratory systems and implications for heterogeneous chemistry in the
686 troposphere", *Physical Chemistry, Chemical Physics*, **6**, 604-613.
687
688 Thomas, W. J., and Crittenden, B. D. (1998) *Adsorption Technology and Design*, Boston,
689 Butterworth-Heinemann.
690
691 Tichenor, B. A., Guo, Z., Dunn, J. E., Sparks, L. E., and Mason, M. A. (1991) "The
692 interaction of vapour phase organic compounds with indoor sinks", *Indoor Air*, **1**, 23-35.
693
694 Wang, J., Huang, C. P., Allen, H. E. (2000) "Surface physical-chemical characteristics of
695 sludge particulates", *Water Environment Research*, **72**, 545-553.
696
697 Webb, A. M., Singer, B. C., and Nazaroff, W. W. (2002) "Effect of gaseous ammonia on
698 nicotine sorption". In: *Proceedings of the 9th International Conference on Indoor Air*
699 *Quality and Climate*, H. Levin, ed., **3**, pp. 512-517.
700
701 Weber, W. J., Jr., and DiGiano, F. A. (1996) *Process Dynamics in Environmental*
702 *Systems*, New York, John Wiley & Sons, Inc.
703
704 Won, D., Corsi, R.L., Rynes, M. (2001) "Sorptive interactions between VOCs and indoor
705 materials", *Indoor Air*, **11(4)**, 246-256.
706

707 **Tables**
708
709

710 Table 1. Langmuir constants and partition coefficients for TMA and NH_3 at different RH

711 values. * These values are based on isotherm data that excludes 0.1 ppm TMA.

712

Sorbate	% RH	Q_a^0 (μg m^{-2})	b (m^3 μg^{-1})	k_e (m)
TMA	20	*200	*2.2 × 10^{-4}	*0.043
	50	98	3.2 × 10^{-4}	0.031
	90	29	4.5 × 10^{-4}	0.013
NH_3	50	196	2.2 × 10^{-4}	0.043

713

714 Table 2. The equilibrium pH of water in contact with air, mixing ratios of carbon dioxide

715 and ammonia, and relative humidity in five residences.

716

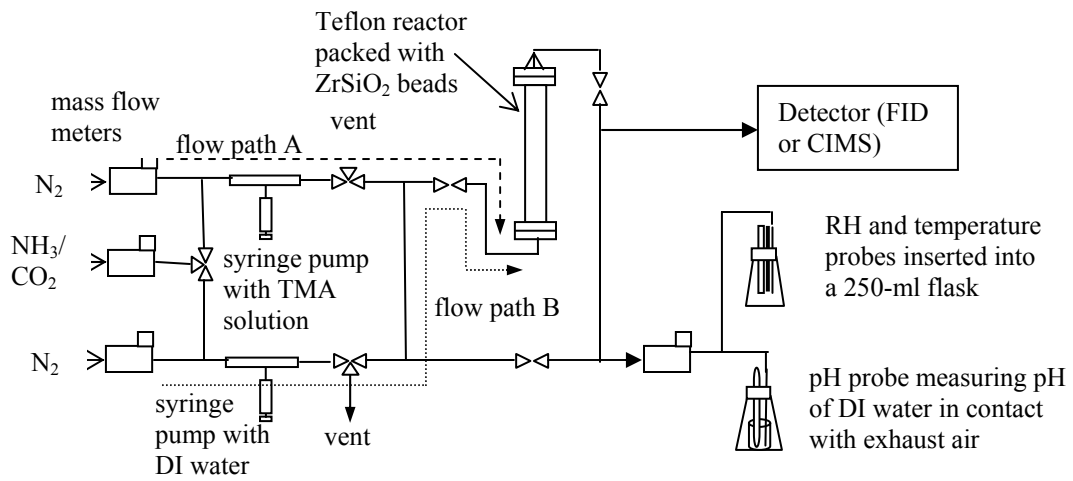| Apartment no.	pH		mean value		
	measured	predicted	CO_2 (ppm)	NH_3 (ppm)	RH (%)
1	5.2	5.4	870	<0.2	50
2	5.2	5.6	510	<0.2	48
3	5.1	5.5	670	<0.2	31
4	5.2	5.6	500	<0.2	26
5	5.0	5.5	710	<0.2	45

717
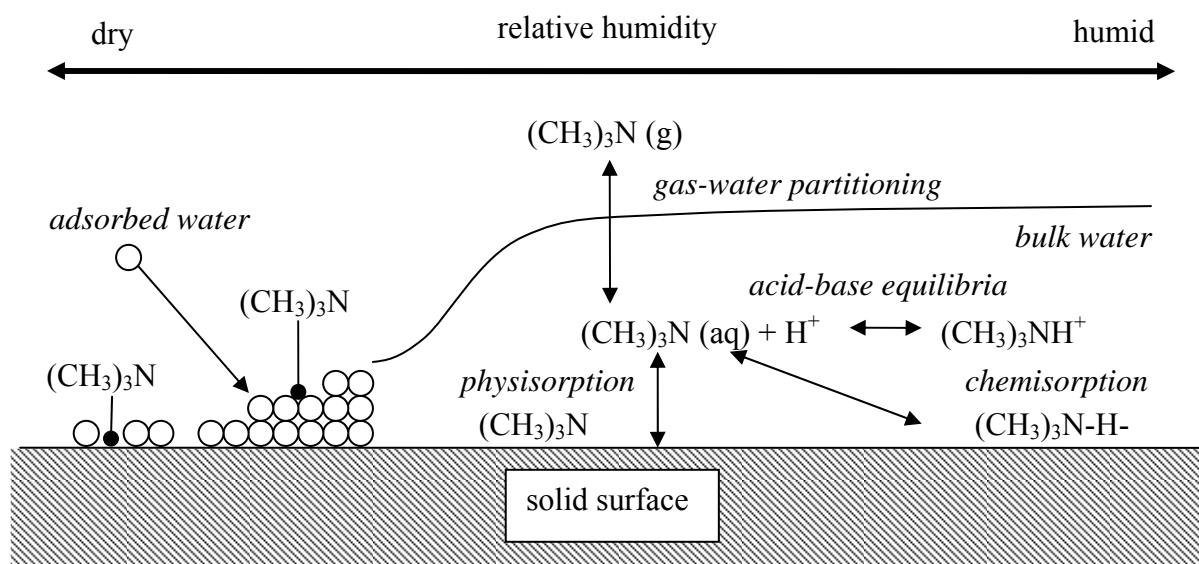
Figures

723   Fig. 1.

724

725
726

727

728

729

730

731

732   Fig. 2
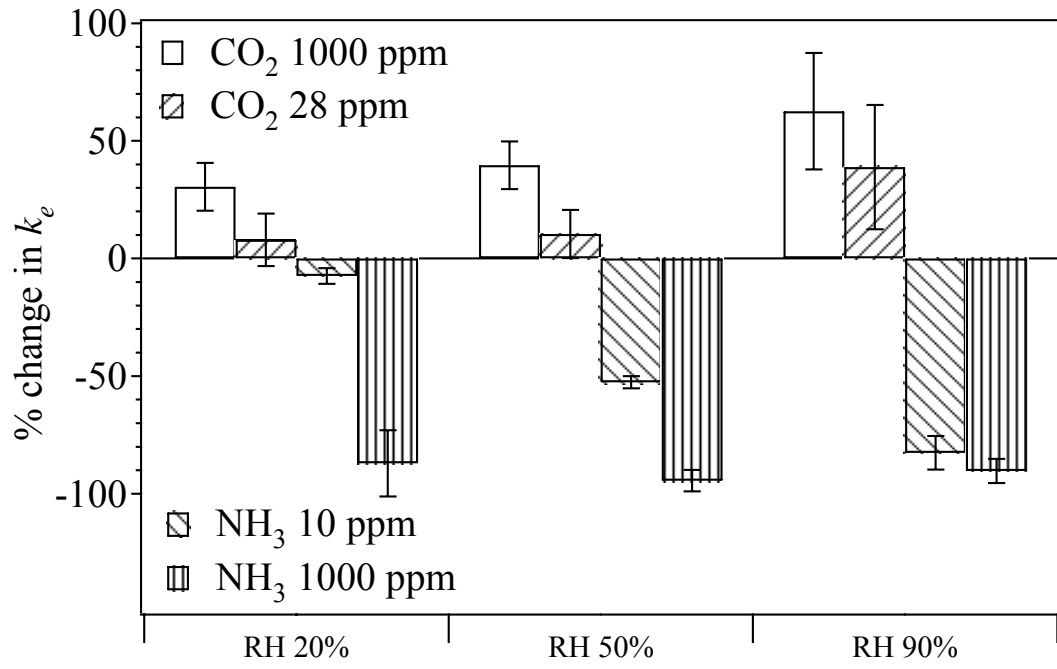
mass flow meters

Teflon reactor packed with ZrSiO$_2$ beads

vent

flow path A

N$_2$

NH$_3$/ CO$_2$

syringe pump with TMA solution

flow path B

N$_2$

syringe pump with DI water

vent

Detector (FID or CIMS)

RH and temperature probes inserted into a 250-ml flask

pH probe measuring pH of DI water in contact with exhaust air

733

734   Fig. 3
735

736

737
738   Fig. 4

739

740
741   Fig. 5

Fig. 6

742
743

744
745
746   Fig. 7
747
748
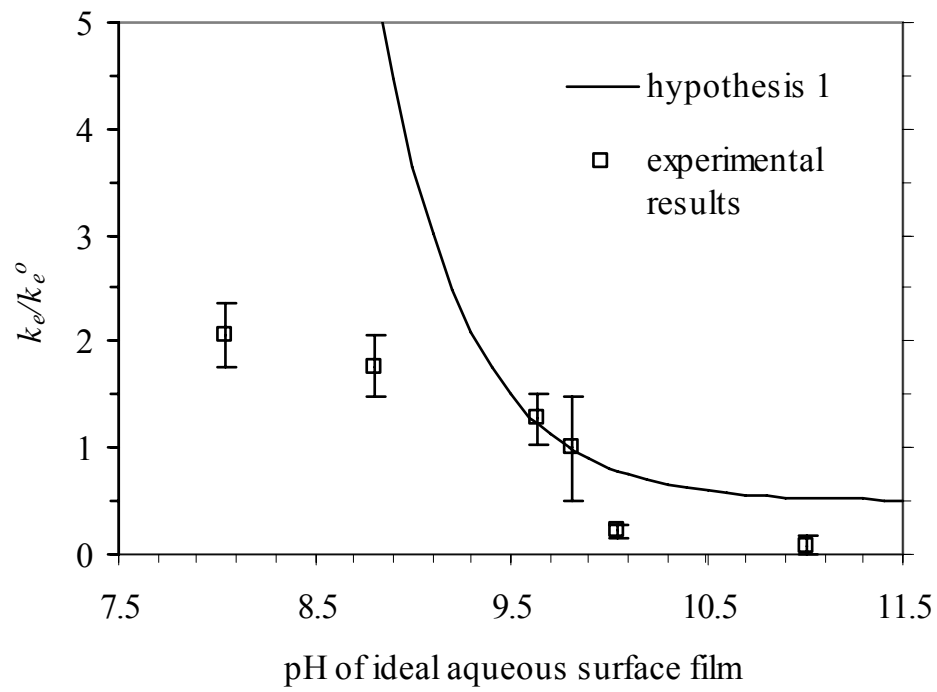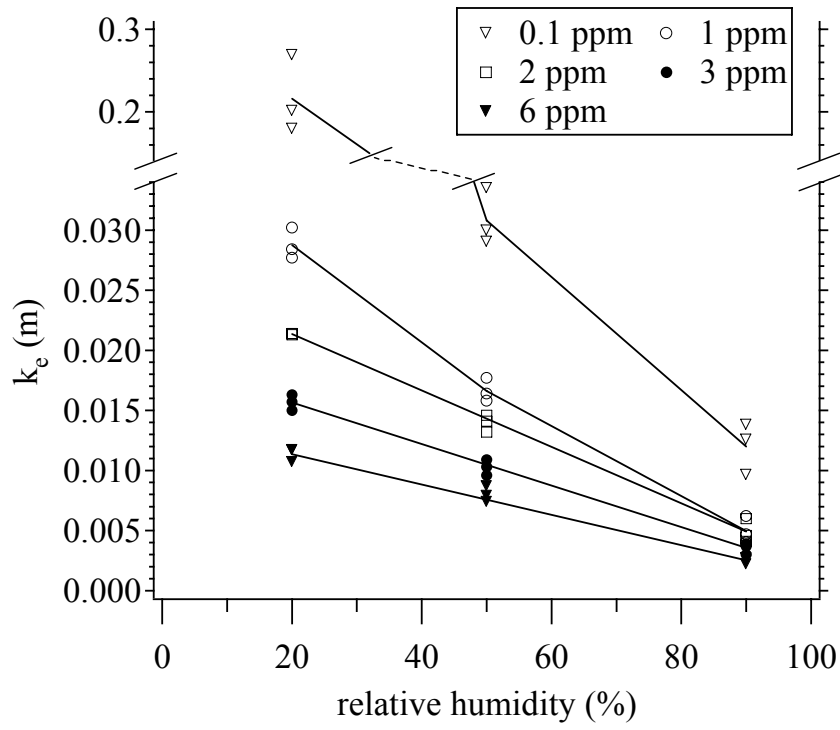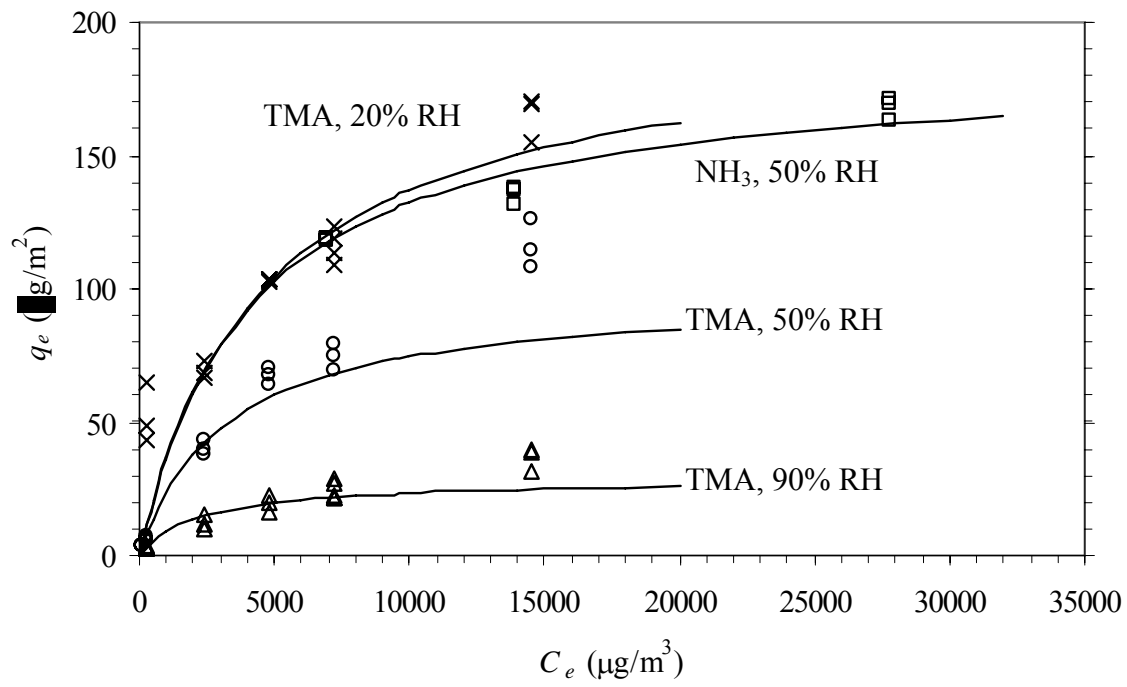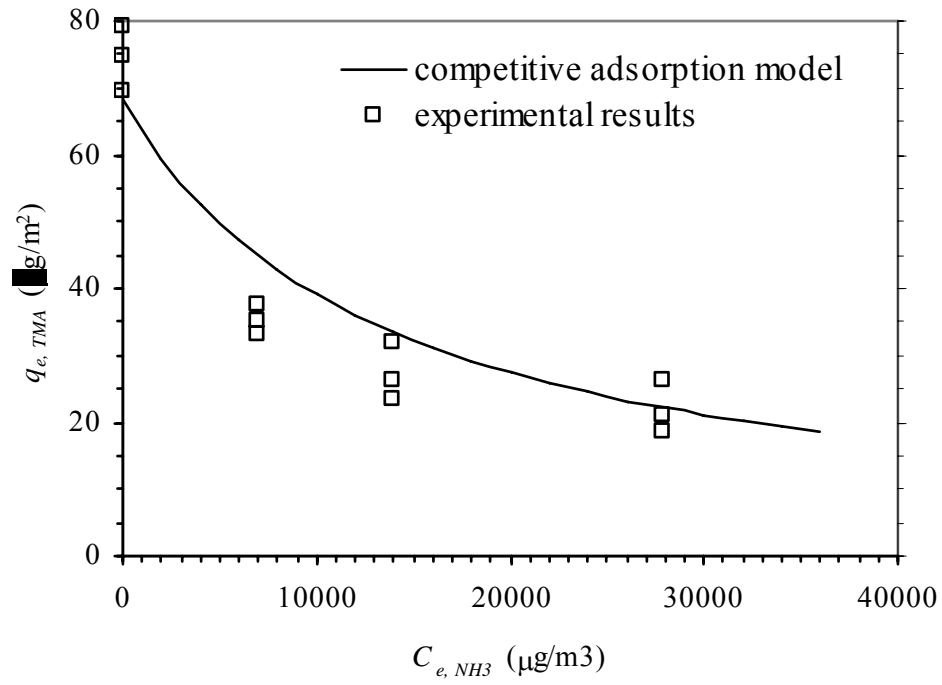
749

750
751
752
753   Fig. 8

754

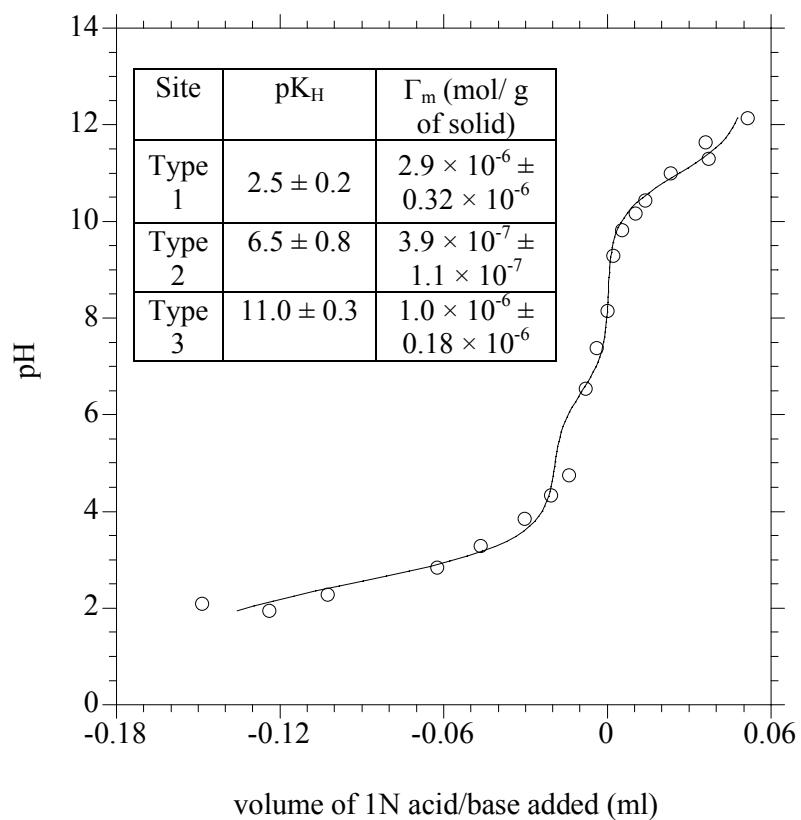| Site	pK$_H$	Γ_m (mol/ g of solid)
Type 1	2.5 ± 0.2	$2.9 \times 10^{-6} \pm 0.32 \times 10^{-6}$
Type 2	6.5 ± 0.8	$3.9 \times 10^{-7} \pm 1.1 \times 10^{-7}$
Type 3	11.0 ± 0.3	$1.0 \times 10^{-6} \pm 0.18 \times 10^{-6}$

volume of 1N acid/base added (ml)
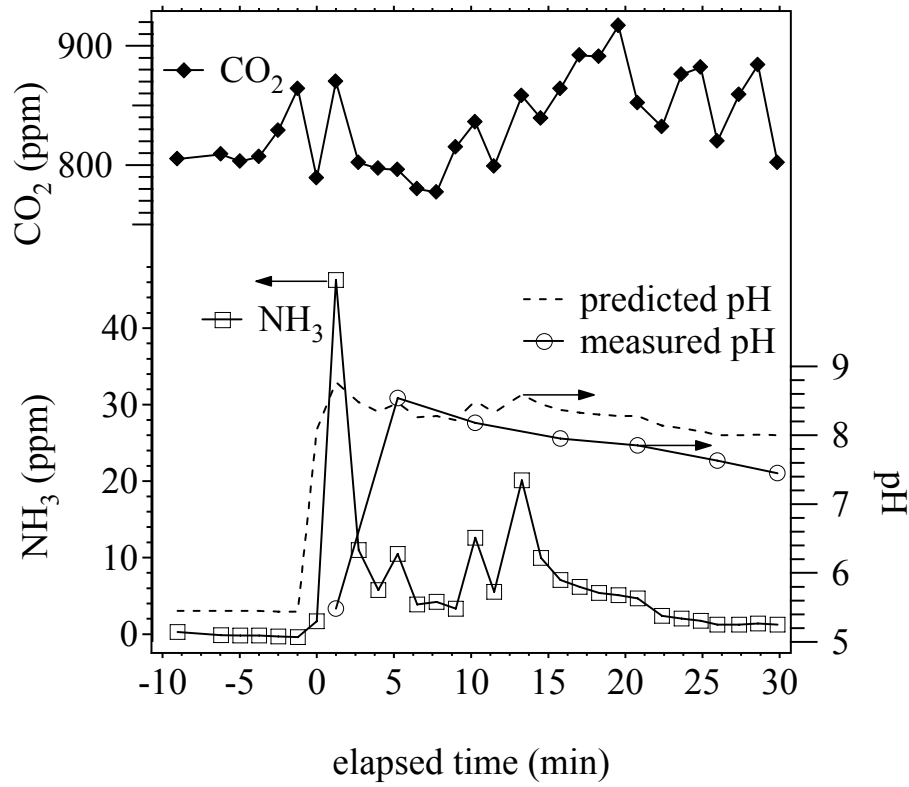
755

756
757   Fig. 9

758
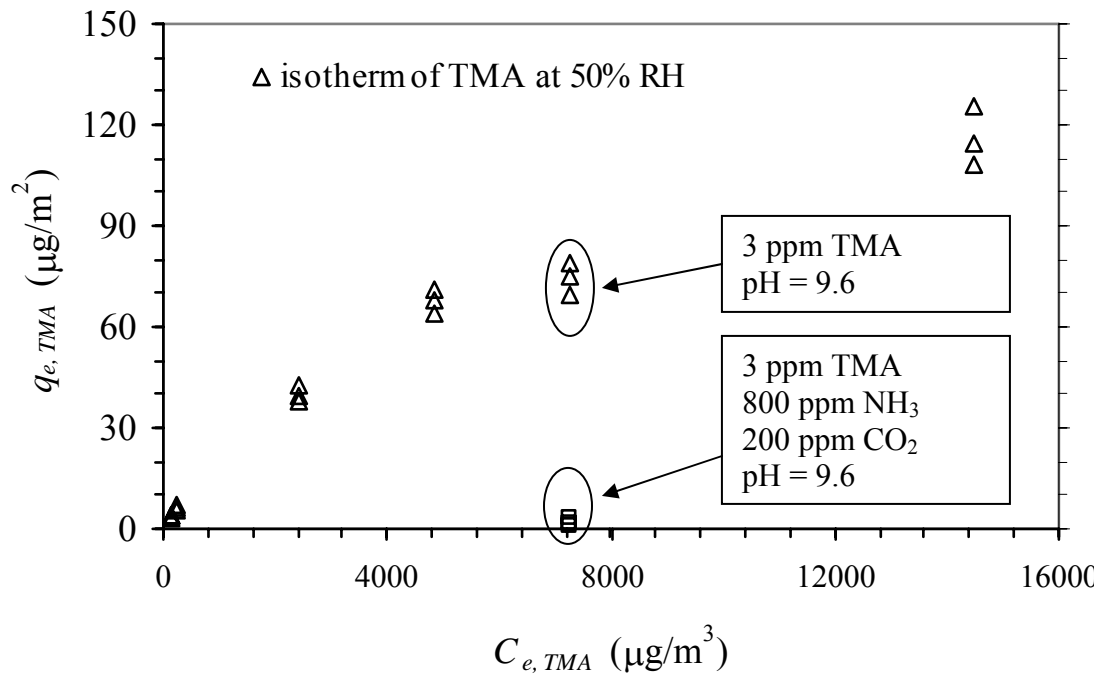
759
760   Figure 10
761

Figure captions

765 Fig. 1. Hypothetical trimethylamine interactions with dry surface, adsorbed water or bulk

766 water.

767 Fig. 2. Experimental apparatus. Aqueous trimethylamine (TMA) is vaporized, diluted and

768 delivered via flow path A to a Teflon plug-flow style reactor packed with zirconium

769 silicate beads. Equilibrium adsorption partition coefficient derived from break-through

770 experiments.

771 Fig. 3. Normalized experimental equilibrium partition coefficient, k_e/k_e^o as the surface pH

772 is modified by either gas-phase ammonia or carbon dioxide. Also shown is the hypothesis

773 1 model prediction considering dissolution and acid-base aqueous chemistry in bulk

774 surface water. Uncertainty range shown is based on error propagation of the standard

775 error from replicate experiments.

776 Fig. 4. Relationship between RH and k_e for trimethylamine mixing ratios ranging from

777 0.1 to 6 ppm.

778 Fig. 5. Percentage change in the equilibrium partition coefficient, k_e, at 20, 50 and 90%

779 RH in the presence of carbon dioxide or ammonia; the trimethylamine mixing ratio is

780 held at 3 ppm. Uncertainty range shown is based on error propagation of the standard

781 error from replicate experiments.

782 Fig. 6. Predicted sorption isotherms (parameters fit to Eq. (5) for single species sorption)

783 of ammonia and TMA at various relative humidity values at 25ºC (solid lines) and

784 experimental results; × for TMA at 20% RH, ○ for TMA at 50% RH, Δ for TMA at 90%

785 RH, and □ for NH_3 at 50% RH.

786   Fig. 7. Predicted competitive adsorption and experimental results obtained from TMA

787   sorption experiments that include ammonia at mixing ratios of 10, 20, and 40 ppm.

788   Fig. 8. The sorptive capacity of TMA in the presence of 800-ppm NH_3 and 200-ppm CO_2

789   ($\square$) compared to the capacity without NH_3 (Δ) at 50% RH.

790   Fig. 9. Titration result for zirconium silicate beads using a solid to liquid ratio of 1:2 and

791   ionic strength of 0.01 M $NaNO_3$.

792   Fig. 10. Measurements of the pH, CO_2 and NH_3 as an ammonia cleaner was applied to a

793   kitchen floor. Also shown is the predicted pH for equilibrium CO_2 and NH_3 partitioning

794   into water.

795